ELSEVIER

PII: S0032-3861(96)00794-X

Polymer Vol. 38 No. 10, pp. 2421–2430, 1997

0032-3861/97/$17.00 + 0.00

A normal mode analysis of form I syndiotactic poly(1-butene)

Tsutomu Ishioka*, Hiroyuki Wakisaka and Isao Kanesaka
Department of Chemistry, Faculty of Science, Toyama University, Gofuku, Toyama 930, Japan

and Motohide Nishimura and Hiroyuki Fukasawa
Department of Material Systems Engineering, Faculty of Technology, Tokyo University of Agriculture and Technology, Koganei, Tokyo 184, Japan
(Received 22 December 1995; revised 10 June 1996)

A normal mode analysis of syndiotactic poly(1-butene) of form I having $(TTGG)_2$ conformation was made in accordance with the valence force field derived by Holland-Moritz for isotactic poly(1-butene) of form I. The assignments were made successfully using polarized infrared and Raman spectra. Based on the assignments, spectral characters in the melt and the low temperature were investigated. The infrared and Raman spectra did not change in the melt but the CCH bendings of the spectra in the low temperature were sensitive to the conformation. © 1997 Elsevier Science Ltd.

(Keywords: syndiotactic poly(1-butene); normal mode analysis; polarized vibrational spectra)

INTRODUCTION

Normal mode analyses of polymers can identify intra- and intermolecular vibrations and characterize them as crystallinity or conformation sensitive bands. Moreover, the analyses can be used to determine rigorous potentials for molecular dynamics or molecular mechanics simulations[1]. Some syndiotactic polymers have been recently synthesized, and found to have different properties from isotactic ones[2–4]. Hence, their vibrations need to be characterized.

Syndiotactic poly(1-butene) (s-PB) has two crystalline forms—forms I and II[4]. Form I is thermodynamically stable and has a fibre period of 7.73 Å. The repeating unit consists of four monomer units having the $(TTGG)_2$ conformation. Form II only exists under tension and has a fibre period of 20.0 Å. The repeating unit consists of 10 monomer units with (5/3) helical symmetry and has a $(T'T'G'G'\ldots)$ conformation where the prime indicates a conformation slightly differing from *trans* or *gauche*.

In contrast, the three crystalline forms I, II and III have been reported for isotactic poly(1-butene). The structure of form I has a hexagonal unit cell containing six 3/1 helices. Form II has a tetragonal unit cell having four 11/3 helices, and form III an orthorhombic unit cell with two 4/1 helices. Vibrational analyses have been reported for isotactic poly(1-butene)[5–9]. Holland-Moritz *et al.*[5] made a normal mode analysis based on the polarized spectra of isotactic poly(1-butene) of form I and its three deuterated derivatives. They used first the valence force constants of normal alkanes[10] and syndiotactic polypropyrene[11] reported by Snyder *et al.* With a slight modification of Snyder's constants, Holland-Moritz *et al.* obtained a reliable set of constants.

In this study we performed a normal mode analysis of s-PB of form I based on the valence force constants of Holland-Moritz *et al.* and checked the transferability of the constants for different tacticity and conformation. Spectral characters in the melt and the low temperature are also discussed.

EXPERIMENTAL

s-PB was supplied from Mitsui Toatsu Chemicals, Inc. The M_n was 27 500 ($M_w/M_n = 1.5$), and the pentad fraction measured by ^{13}C n.m.r. was 0.91. The uniaxially oriented specimen of form I was obtained by stretching the film obtained from the melt in ice water. The structure was confirmed by X-ray diffraction. The polarized infrared measurements were made by a JASCO IR-810 or a JEOL JIR-100 *FT* i.r. spectrophotometer at room temperature. The polarized Raman measurements were carried out at room temperature by a JASCO R-800 double monochromator with an Ar^+ laser (514.5 nm) providing the incident light. The temperature dependence of the infrared and Raman spectra was recorded with a JASCO IR-810 spectrophotometer and an R-800 double monochromator, respectively.

RESULTS AND DISCUSSION

Isotactic poly(1-butene) of form II can be obtained by cooling from the melt. Form II is transformed into form I by annealing. From III is prepared by casting from decalin, benzene, *p*-xylene, toluene or carbon tetrachloride. Hence, the different forms were obtained by different preparation methods. We checked these in s-PB. The infrared spectra of s-PB cast from five different solvents, chloroform, benzene, xylene, toluene

* To whom correspondence should be addressed

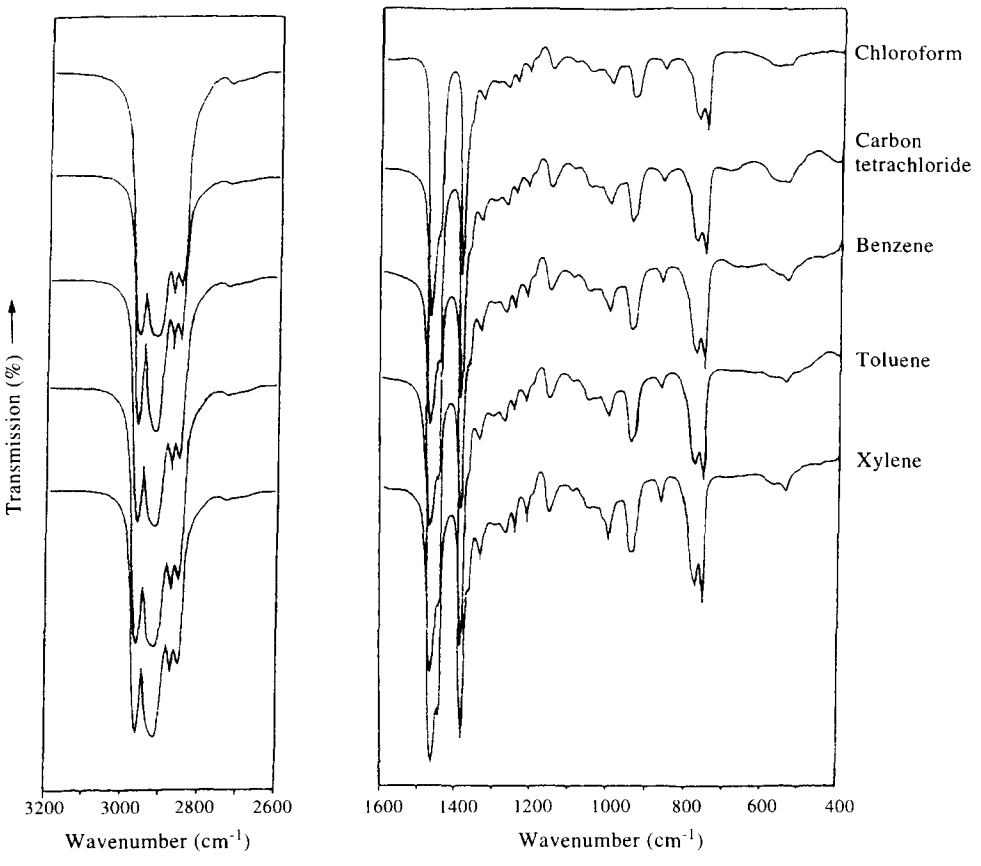

Figure 1 Infrared spectra of s-PB films cast from different solvents in the 400–1600 cm^{-1} and 2600–3200 cm^{-1} regions

and carbon tetrachloride, reveal the same spectral patterns, as shown in *Figure 1*, which also coincide with the spectrum of s-PB of form I obtained by cooling from the melt. Hence, these preparation methods result in the same structure of form I.

We performed a normal mode analysis of form I by the Wilson GF matrix method using an IBM RS/6000-580 computer. All angles were assumed to be tetrahedral, and the C–C and C–H bond lengths were 1.54 and 1.093 Å, respectively. The molecular symmetry of the s-PB of form I belongs to the D_2 line group. The matrix related to the 160 internal coordinates were factored into 42A, $40B_1$, $40B_2$ and $38B_3$ blocks by using the symmetry coordinates (*Table 1*) reported by Snyder for syndiotactic polypropylene[11]. Each block has 35 genuine vibrations. All diagonal and off-diagonal force constants were transferred from those of Holland-Moritz and are listed in *Table 2*[5]. Those of Snyder[11] were also examined, and the results are described below. The resultant calculated frequencies according to Holland-Moritz's force constants and the observed frequencies are listed in *Table 3*. The agreement between the calculated and observed frequencies is good. The potential energy distributions of the bands except for the C–H stretches were mixed with several modes. The wavenumbers and the potential energy distributions of the CCH bendings of the CH_2 groups depend on the difference of the skeletal conformations by referring the normal mode analyses of isotactic PB[5,6].

The molecular symmetry of the s-PB of form I is the D_2 line group. The z axis is taken to be the molecular axis of the chain. Hence, in the polarized infrared spectra, the B_3 mode is parallel to the chain. The B_1 and B_2 modes are perpendicular. Since we have a one-dimensionally oriented specimen, we cannot distinguish the B_1 and B_2 modes in the polarized spectra. The A modes are infrared inactive. *Figure 2* shows the polarized infrared spectra of s-PB in the 600–1600 cm^{-1} region.

The strongest bands at about 1460 cm^{-1} are assigned to CH_3 asymmetric bendings α_a and α_b, plus CH_2 bendings of the main chain δ(m) and side chain δ(s). The 1441 cm^{-1} band having perpendicular polarization is also assigned to δ(m) and δ(s). Because of the vibrational coupling between δ and α, these modes are not clearly separated. The 1381 cm^{-1} band in both parallel and perpendicular polarizations is the CH_3 symmetric bend U^-, and the 1360 cm^{-1} band of parallel polarization is U^- plus CH_2 wagging of the main chain W(m). The 1331 cm^{-1} band of parallel polarization is W(s). The weak parallel bands at 1290 and 1267 cm^{-1} are assigned to W(m) and CH_2 twisting of the side chain T(s). The 1242 cm^{-1} band of parallel polarization is W(m). The 1209 cm^{-1} band of perpendicular polarization is assigned to T(m) or the CH bend ξ_b. The 1155 cm^{-1} band is ξ_b, and the 1149 cm^{-1} band may be T(m). The 995 cm^{-1} band of perpendicular polarization is assigned to the C–CH_3 stretch R or CC stretch of the main chain S(m). The two bands of parallel polarization at 941 and 931 cm^{-1} are ascribed to R, although we have only one calculated frequency. The parallel bands at 864 and 775 cm^{-1} are CH_2 rocking of the main chain P(m) and the side chain P(s), respectively. The 754 cm^{-1} band of perpendicular polarization is CC stretching of the side chain S(s) of the B_1 mode. No calculated frequency of the intramolecular mode corresponds to the two fairly strong bands at 694 and 617 cm^{-1}. These bands may be experimental artifacts

Table 1 Group coordinates of s-PB of form I

Coordinate	Symbol	Description
$2r_1 - r_2 - r_3$	r_a^-	CH_3 asym. C–H stretch
$r_2 - r_3$	r_b^-	CH_3 asym. C–H stretch
$r_1 + r_2 + r_3$	r^+	CH_3 sym. C–H stretch
$d(m)_1 + d(m)_2$	$d(m)^+$	CH_2 sym. C–H stretch (amin chain)
$d(m)_1 - d(m)_2$	$d(m)^-$	CH_2 asymm. C–H stretch (main chain)
s	s	CH C–H stretch
$S(m)_1 + S(m)_2$	$S(m)^+$	C–C skeletal stretch (main chain)
$S(m)_1 - S(m)_2$	$S(m)^-$	C–C skeletal stretch (main chain)
R	R	C–CH_3 stretch
$\alpha_1 + \alpha_2 + \alpha_3 - \beta_1 - \beta_2 - \beta_3$	U^-	CH_3 sym. bend
$2\alpha_1 - \alpha_2 - \alpha_3$	α_a	CH_3 asym. bend
$\alpha_2 - \alpha_3$	α_b	CH_3 asym. bend
T	T	C–CH_3 torsion
$2\beta_1 - \beta_2 - \beta_3$	β_a	CH_3 rock
$\beta_2 - \beta_3$	β_b	CH_3 rock
$\delta(m)$	$\delta(m)$	CH_2 bend (main chain)
$\gamma(m)_1 + \gamma(m)_2 + \gamma(m)'_1 + \gamma(m)'_2$	$\Gamma(m)$	CH_2 bend (main chain)
$\gamma(m)_1 + \gamma(m)_2 - \gamma(m)'_1 - \gamma(m)'_2$	$W(m)$	CH_2 wag (main chain)
$\gamma(m)_1 - \gamma(m)_2 - \gamma(m)'_1 + \gamma(m)'_2$	$T(m)$	CH_2 twist (main chain)
$\gamma(m)_1 - \gamma(m)_2 + \gamma(m)'_1 - \gamma(m)'_2$	$P(m)$	CH_2 rock (main chain)
$2\zeta_1 - \zeta_2 - \zeta_3$	ζ_a	CH bend
$\zeta_2 - \zeta_3$	ζ_b	CH bend
$\zeta_1 + \zeta_2 + \zeta_3$	ζ^+	C–C–C bend
$2\phi_1 - \phi_2 - \phi_3$	ϕ_a	C–C–C bend (main chain)
$\phi_2 - \phi_3$	ϕ_b	C–C–C bend
$\phi_1 + \phi_2 + \phi_3$	ϕ^+	C–C–C bend
$\tau(m)_1 + \tau(m)_2$	$\tau(m)^+$	CH_2–CH torsion (main chain)
$\tau(m)_1 - \tau(m)_2$	$\tau(m)^-$	CH_2–CH torsion (main chain)
$\alpha_1 + \alpha_2 + \alpha_3 + \beta_1 + \beta_2 + \beta_3$	U^+	redundant
$d(s)_1 + d(s)_2$	$d(s)^+$	CH_2 sym. C–H stretch (side chain)
$d(s)_1 - d(s)_2$	$d(s)^-$	CH_2 asymm. C–H stretch (side chain)
$S(s)$	$S(s)$	C–C skeletal stretch (side chain)
$\delta(s)$	$\delta(s)$	CH_2 bend (side chain)
$\omega(s)$	$\omega(s)$	C–C–C bend (side chain)
$\tau(s)$	$\tau(s)$	CH_2–CH torsion (side chain)
$\gamma(s)_1 + \gamma(s)_2 + \gamma(s)'_1 + \gamma(s)'_2$	$\Gamma(s)$	CH_2 bend (side chain)
$\gamma(s)_1 + \gamma(s)_2 - \gamma(s)'_1 - \gamma(s)'_2$	$W(s)$	CH_2 wag (side chain)
$\gamma(s)_1 - \gamma(s)_2 - \gamma(s)'_1 + \gamma(s)'_2$	$T(s)$	CH_2 twist (side chain)
$\gamma(s)_1 - \gamma(s)_2 + \gamma(s)'_1 - \gamma(s)'_2$	$P(s)$	CH_2 rock (side chain)

Asym., asymmetric; sym., symmetric

arising from the signal-to-noise ratio. For the CH stretches in the 2800–2900 cm^{-1} region, the assignments are clear, since the vibrational coupling between these modes is small. The 2964 cm^{-1} band is ascribed to CH_3 asymmetric stretches r_a^- and r_b^-, the 2930 cm^{-1} band is CH_2 asymmetric stretching of the main chain $d(m)^-$, the 2916 cm^{-1} band is CH_2 asymmetric stretching of the side chain $d(s)^-$, the 2875 cm^{-1} band is CH_3 symmetric stretching r^+, the 2854 cm^{-1} band is CH_2 symmetric stretching of the main and the side chains $d(s)^+$ plus $d(m)^+$. The calculated frequencies at 2903 and 2902 cm^{-1} of CH stretches s are not clearly observed.

In the polarized Raman spectra of s-PB, the A, B_1, B_2, and B_3 modes are all Raman active. The bands in the zz and xx polarizations are assigned to the A modes. The xz polarization is assigned to the B_1 or B_2 modes, and the xy polarization to the B_3 mode. The A modes are Raman active but infrared inactive. Hence, the bands appearing only in the Raman spectra are assigned to the A modes.

Figure 3 shows the polarized Raman spectra in the 200–2000 and 2600–3200 cm^{-1} regions. As in the case of the infrared spectra, the characteristic feature appears in the 600–1600 cm^{-1} region. We start from the assignments of the A modes. The strongest bands appearing at 1445 and 1465 cm^{-1} are assigned to $\delta(s)$, and $\delta(m)$ plus α_a and α_b. The calculated frequencies of these modes are too close to be assigned separately. A broad spectral feature appeared at 1250–1400 cm^{-1}. There are five calculated frequencies in this region. Of these, the weak band at 1378 cm^{-1} is assigned to U^-, the main band at 1327 cm^{-1} to $W(s)$, and the sharp 1284 cm^{-1} band appearing in the xx polarization to $T(s)$. No clear peak corresponds to the calculated frequencies at 1350 and 1371 cm^{-1} of ζ_a and ζ_b. In the 900–1200 cm^{-1} region, five

Table 2 Valence force constants of s-PB of form I

Diagonal	Value	Interaction	Value	Interaction	Value
K_R	4.329	F_r	0.029	f_β^g(s)	−0.043
K_S(m)	4.337	F_d(s)	0.016	$f_{\beta\gamma}^{t}$(m)	0.002
K_S(s)	4.337	F_d(m)	0.006	$f_{\beta\gamma}^{t}$(s)	−0.002
K_d(m)	4.554	F_R(m)	0.101	$f_{\beta\gamma}^{g}$(m)	0.009
K_d(s)	4.546	F_R(s)	0.064	$f_{\beta\gamma}^{g}$(s)	0.002
K_s	4.588	$F_{R\beta}$(m)	0.328	$f_\gamma^{''t}$(m)	−0.014
K_r	4.699	$F_{R\beta}$(s)	0.261	$f_\gamma^{''g}$(m)	−0.025
H_α	0.54	$F'_{R\gamma}$(m)	0.079	$f_{\beta\omega}^{t}$(m)	0.049
H_β	0.637	$F'_{R\gamma}$(s)	−0.004	$f_{\beta\omega}^{t}$(s)	0.072
H_γ(m)	0.66	$F_{R\omega}$(m)	0.417	$f_{\beta\omega}^{g}$(m)	−0.052
H_γ(s)	0.666	$F_{R\omega}$(s)	0.351	$f_{\beta\omega}^{g}$(s)	−0.058
H_δ(m)	0.55	F_β(s)	−0.017	f_ω^t	−0.011
H_δ(s)	0.55	F_γ(m)	−0.021	f_ω^g	0.011
H_ω(m)	1.13	F'_γ(m)	0.041	F_ω	−0.041
H_ω(s)	0.901	F'_γ(s)	0.023		
H_ϕ	1.084	$F_{\gamma\omega}$(m)	−0.031		
H_ζ	0.657	$F_\gamma\omega$(s)	−0.124		
H_τ(m)	0.024	f_β^t(m)	0.127		
H_τ(s)	0.024	f_β^t(s)	0.088		
H_T	0.024	f_β^g(m)	−0.005		

(m) and (s) denote main chain and side chain, respectively. Stretch constants are in mdyn Å^{-1} and bend constants are in mdyn Å^{-1} rad^{-2}, and stretch–bend interaction constants are in mdyn rad^{-1}

bands appeared, and are ascribed to the coupled modes as shown in *Table 3*. In the *zz* polarization, a clear singlet appeared at 845 cm^{-1}, whereas in the *xx* polarization two weak peaks at 830 and 860 cm^{-1} appeared in the same region. The band in the *zz* polarization is assigned to *S*(m), whereas the weak bands in the *xx* polarization may be ascribed to *P*(m) in the B_1, B_2 or B_3 species. The band at 787 cm^{-1} is assigned to *P*(s). Several side bands appearing around 770 cm^{-1} may be due to leakage from the other species. The assignments of the CH stretches in the 2600–3200 cm^{-1} region were unambiguous, as was the case for the infrared spectra.

For the B_1, B_2, and B_3 modes, the assignments and the spectral feature are not so different from those of the A modes, since similar modes appear in each polarization. Since the observed intensities of these modes were weak, only assignments for fairly intense bands were made, as shown in *Table 3*. We also calculated the frequencies using Snyder's force constants[11] of H_γ(m) = 0.655 mdyn Å^{-1} rad^{-2}, F'_γ(m) = 0.012, f_β^t(s) = 0.106 and f_β^g(s) = −0.024. Holland-Moritz used a real molecular geometry with a CCC angle of 114° in the main chain, while Snyder used a tetrahedral angle. Hence, differences may appear mainly in the modes of such as *W*(s), *W*(m), *T*(s), *T*(m), *P*(s) and *P*(m) involving CCH bendings of the main chain and the CCC bendings of the main chain. Since just a few observed frequencies are available for the CCC bendings, a comparison between only the above CCH

Table 3 Observed and calculated frequencies (cm^{-1}), and potential energy distribution (%) of s-PB of form I

$\nu_{calc.}$	$\nu_{obs.}$ I.r.	Relative intensity	$\nu_{obs.}$ Raman	Relative intensity[a]	Potential energy distribution[b]
A modes					
2966			2958	vs	r_a^- 74, r_b^- 24
2966			2958	vs	r_a^- 25, r_b^- 75
2922			2933	vs	d(s)$^-$ 98
2904			2904	vs	s 99
2874			2875	vs	r^- 99
2856			2853	vs	d(m)$^+$ 86, d(s)$^+$ 13
2856			2853	vs	d(s)$^+$ 84, d(m)$^+$ 10
2854			2853	vs	d(m)$^+$ 99
1467			1465	sh	α_a 71, α_b 19
1466			1465	sh	α_b 36, δ(s) 30
1464			1465	sh	δ(m) 65, Γ(m) 30
1461			1465	sh	δ(m) 59, Γ(m) 15, α_b 13
1455			1445	vs	δ(s) 42, α_b 16, δ(m) 14, Γ(s) 12
1375			1378	w	U^- 80
1371					ζ_b 28, S(m)$^-$ 23, T(s) 14, T(m) 12
1350					ζ_a 31, S(s) 22, T(m) 14
1326			1327	m	W(s) 53, S(s) 14, R 12
1263			1284	m	T(s) 57, ζ_b 16
1241					T(m) 57, S(m)$^-$ 11
1202					S(m)$^-$ 19, P(s) 18, T(m) 13, β_a 12
1144			1151	m	ζ_a 37, T(m) 16, β_a 10, R 10
1058			1070	w	T(m) 42, ζ_b 25, S(s) 10
1028			1046	m	β_a 20, R 18, β_b 12, ζ_a 12
989			995	w	S(m)$^-$ 25, T(s) 22, β_b 19
940			940	w	R 32, β_b 16, S(m)$^+$ 16
811			845	m	S(m)$^+$ 24, S(s) 24, ω(m) 12, R 11
772			787	w	P(s) 52, β_a 28
581					S(s) 24, ω(m) 14, ϕ_a 11
439					ω(m) 26, S(m)$^+$ 21, ω(s) 20, S(s) 11,
300					ϕ_a 31, ϕ_b 17, S(m)$^-$ 12, ω(m) 12, S(m)$^+$ 10

Table 3 Continued

$\nu_{calc.}$	$\nu_{obs.}$ I.r.	Relative intensity	$\nu_{obs.}$ Raman	Relative intensity[a]	Potential energy distribution[b]
190			208	m	ω(s) 27, ω(m) 24
160					ω(m) 26, ϕ^+ 19, ζ^+ 14, ω(s) 10, ϕ_a 12
109					T 89
40					ϕ_b 37, ω(m) 29, ϕ_a 13
32					τ(s) 94
B_1 modes					
2966	2964	vs	2953	vs	r_a^- 74, r_b^- 24
2966	2964	vs	2953	vs	r_b^- 75, r_a^- 25
2929	2930	vs	2926	vs	d(m)$^-$ 96
2922	2916	vs	2926	vs	d(s)$^-$ 98
2903			2898	vs	s 96
2874	2875	vs	2870	vs	r^+ 99
2856	2854	vs	2860	vs	d(s)$^+$ 80, d(m)$^+$ 16
2855	2854	vs	2860	vs	d(m)$^+$ 80, d(s)$^+$ 18
1467			1463	sh	α_a 70, α_b 20
1466	1464	s	1463	sh	δ(s) 32, δ(m) 28, α_b 15, Γ(s) 10
1464	1461	s	1463	sh	α_b 38, δ(m) 27, α_a 14
1455	1441	s	1448	vs	δ(m) 17, α_b 16
1392					S(m)$^-$ 20, ζ_b 19, W(m) 14, S(m)$^+$ 12,
1374	1381	s	1378	w	U^- 84
1364					ζ_b 18, ϕ_b 18, W(m) 15, T(m) 14, S(s) 14
1329			1335	m	W(s) 54, ζ_a 15, R 13
1264	1265	w			T(s) 56
1235					W(m) 42, ζ_a 12
1209	1209	m	1203	w	T(m) 27, S(m)$^+$ 16, P(m) 11
1170					ζ_a 37, β_a 11
1118					ζ_b 23, T(m) 18, S(m)$^-$ 12
1024	1030	w			ζ_a 32, R 30, β_a 22
1013	1012	w			S(m)$^-$ 35, T(s) 23, β_a 19
990	995	m	1003	w	R 19, β_a 18, W(s) 15, P(m) 10
864	864	m	846	w	P(m) 33, R 20, S(s) 19
794			788	w	P(s) 36, β_a 20, β_b 15
756	754	s			S(s) 22, S(m)$^+$ 20, P(m) 16
570	566	w			ϕ^+ 19, ζ^+ 14
480					ϕ_a 38, ω(m) 18, ω(s) 11, P(s) 10
260					ϕ_b 34, ϕ^+ 16, ζ^+ 11, ω(s) 11
175					ω(s) 24, ϕ_b 22, ϕ_a 19
166					ω(m) 31, ϕ_a 19, ϕ_b 11, S(m)$^+$ 10
109					T 89
32					τ(s) 94
28					τ(m)$^-$ 91
B_2 modes					
2966	2964	vs	2953	vs	r_a^- 75, r_b^- 24
2966	2964	vs	2953	vs	r_b^- 76, r_a^- 24
2930	2930	vs	2926	vs	d(m)$^-$ 91
2922	2916	vs	2926	vs	d(s)$^-$ 92
2903			2898	vs	s 96
2874	2875	vs	2870	vs	r^+ 99
2856	2854	vs	2860	vs	d(s)$^+$ 94
2855	2854	vs	2860	vs	d(m)$^+$ 94
1468	1464	s	1463	sh	α_a 70, α_b 18
1466			1463	sh	α_b 41, δ(s) 22, δ(m) 15
1463	1461	s	1463	w	δ(m) 55, Γ(m) 17
1456	1441	s	1448	vs	δ(s) 48, α_b 24, Γ(s) 14
1401					S(m)$^-$ 35, ζ_b 19, W(m) 13
1375	1381	s	1378	w	U^- 84
1343					ζ_a 43, W(s) 13, U^- 10, S(s) 10

Table 3 Continued

$\nu_{calc.}$	$\nu_{obs.}$ I.r.	Relative intensity	$\nu_{obs.}$ Raman	Relative intensity[a]	Potential energy distribution[b]
1319			1319	m	W(s) 40, S(s) 27
1282			1286	w	W(m) 42, T(m) 31
1263					T(s) 62, ζ_b 13
1209	1209	m	1203	w	ζ_b 32, $S(m)^-$ 14, P(s) 14, β_a 11
1143	1149	m	1153	m	T(m) 30, W(m) 19, ζ_b 18, $S(m)^-$ 10,
1112	1113	w	1093	w	R 28, ζ_a 24, S(s) 10
1041	1043	w	1046	m	β_a 21, W(s) 16, T(m) 14, ζ_a 10
998	995	m	1003	w	$S(m)^-$ 25, T(s) 24, β_a 22
933	931	m	945	w	$S(m)^+$ 29, P(m) 23
925					R 45, β_a 16, $S(m)^+$ 16
820					P(m) 20, $S(m)^+$ 19, S(s) 19, β_a 10
765	775	s	788	w	P(s) 50, β_a 21
537	538	m			ω(s) 26, P(m) 16, ϕ^+ 16, ζ^+ 12
448	443	w			ϕ_b 30, S(s) 20, ω(m) 13
301					ϕ_a 38, ω(s) 18
204					ϕ_a 30, ω(s) 21, ϕ^+ 11
153					ω(m) 29, ϕ_b 27, T 11
108					T 84
37					τ(s) 80
22					$\tau(m)^+$ 81, τ(s) 12
B_3 modes					
2966	2964	vs	2953	vs	r_a^- 76, r_b^- 23
2966	2964	vs	2953	vs	r_b^- 76, r_a^- 23
2930	2930	vs	2935	vs	$d(m)^-$ 91
2929	2930	vs	2935	vs	$d(m)^-$ 96
2922	2916	vs	2915	vs	$d(s)^-$ 92
2902			2880	vs	s 94
2874	2875	vs	2880	vs	r^+ 99
2856	2854	vs	2855	vs	$d(s)^-$ 98
1467	1464	s	1465	sh	α_a 68, α_b 23
1465	1461	s	1465	sh	α_b 41, δ(s) 29, α_a 15
1456			1449	vs	δ(s) 46, α_b 25, Γ(s) 13
1403					$S(m)^-$ 42, ζ_b 23, W(m) 17
1377	1381	s	1376	w	U^- 58, ζ_a 10
1368	1360	m			U^- 27, W(m) 24, S(s) 13, $S(m)^+$ 12, ζ_a 11
1329	1331	m	1334	m	W(s) 53, R 13, ζ_a 10
1292	1290	w	1314	w	W(m) 57, ζ_b 20
1261	1267	w			T(s) 64, β_a 10, ζ_b 10
1220	1242	m			W(m) 34, ζ_a 28
1183	1155	m	1150	m	ζ_b 25, β_a 13, $S(m)^-$ 14, P(s) 10
1107	1113	w			$S(m)^+$ 22, W(m) 19, S(s) 13, W(s) 13, ζ_a 12
1066	1066	w	1051	w	R 26, β_b 19, P(m) 14
1017	1024	w			$S(m)^-$ 30, T(s) 25, β_a 22, P(s) 10
988	997	m	1000	w	β_b 23, $S(m)^+$ 16, P(m) 16, W(s) 16, β_a 11
	941	m			
924	931	m			R 47, P(m) 19, ζ_a 12
864	864	m			P(m) 52, $S(m)^+$ 21, ζ_b 12
804					S(s) 39, P(m) 25, $S(m)^+$ 11
782	775	s	793	w	P(s) 47, β_a 24, β_b 12
528	538	m			ω(s) 23, ϕ^+ 20, P(m) 16, ζ^+ 14
393					ϕ_b 53, ϕ_a 14
349					ϕ_a 54
227			210	m	ω(s) 34, ϕ^- 15, ϕ_b 13, ζ^+ 11
115					T 96
55					τ(s) 64, $\tau(m)^-$ 29
37					$\tau(m)^+$ 53, $\tau(m)^-$ 35
21					$\tau(m)^+$ 39, $\tau(m)^-$ 33, τ(s) 26

[a] v, very; s, strong; m, medium; w, weak; sh, shoulder
[b] Potential energy distributions less than 10% were neglected. Symbols are the same as in *Table 1*. (m) and (s) denote main chain and side chain, respectively

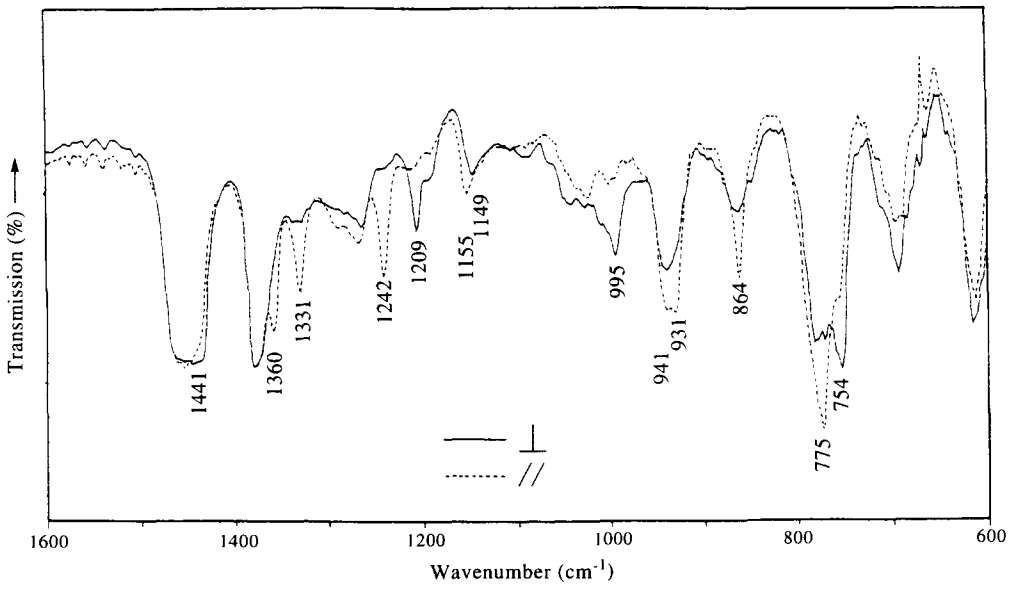

Figure 2 Polarized infrared spectra of s-PB of form I: ——, electric vector perpendicular to the orientation direction which corresponds to B_1 and B_2 modes of T% from 20 to 40; · · ·, parallel to the orientation direction which corresponds to B_3 modes of T% from 10 to 30

bending modes is listed in *Table 4*. The difference between the calculated results was slight, but complicated because of the close coupling between modes.

There are no appreciable differences in the spectra between the stretched and non-stretched specimens. Both specimens have a degree of crystallinity of about a few tens of per cent as estimated by an X-ray diffraction. In the case of isotactic poly(1-butene) of form I, the crystallinity sensitive bands appear at 1222 cm^{-1} T(m), 1207 cm^{-1} T(m), 924 cm^{-1} β_b and 848 cm^{-1} β_b[7]. Corresponding bands

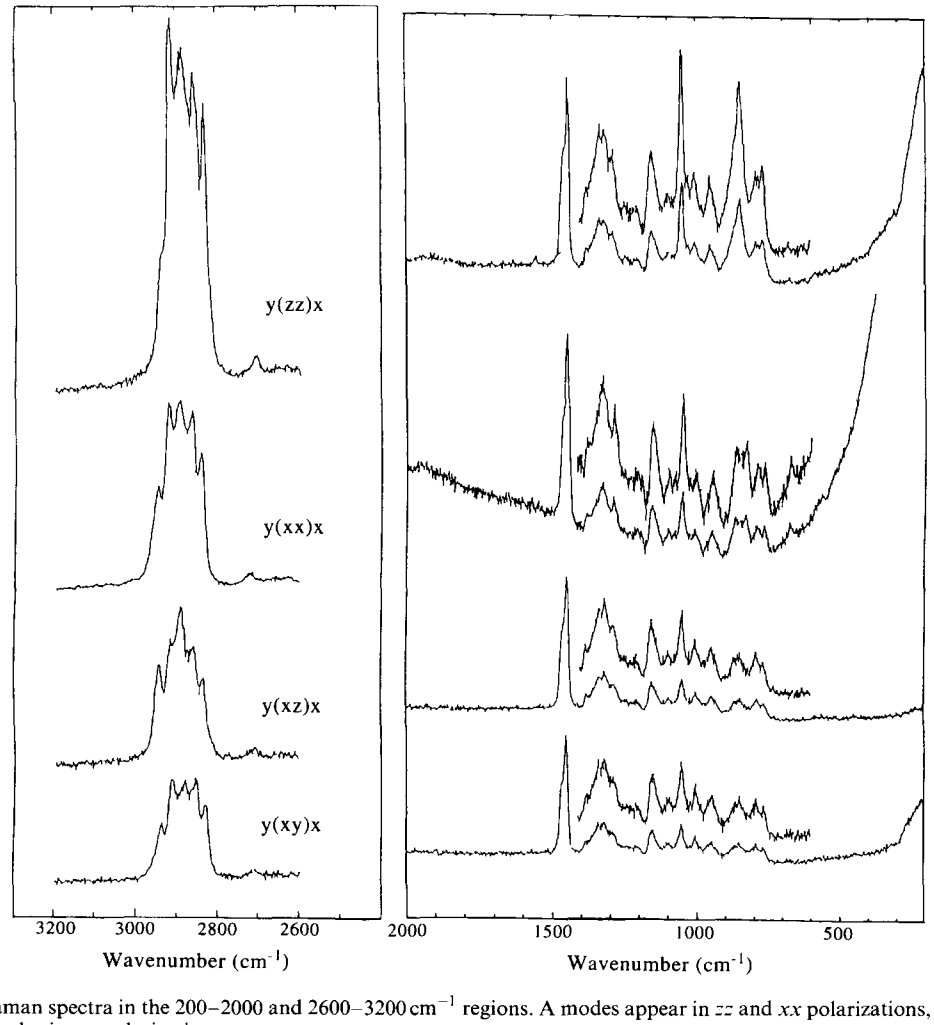

Figure 3 Polarized Raman spectra in the 200–2000 and 2600–3200 cm^{-1} regions. A modes appear in zz and xx polarizations, B_1 and B_2 modes in xz polarization, and B_3 modes in xy polarization

Table 4 Comparison between calculated frequencies (cm^{-1}) using the force constants of Holland-Moritz and Snyder. The observed frequencies of infrared and Raman spectra are also listed

$\nu_{calc.}$ and potential energy distribution (%)				$\nu_{obs.}$	
Holland-Moritz		Snyder		Infrared	Raman
A modes					
1326	*W*(s) 53[a]	1326	*W*(s) 52		1327
1263	*T*(s) 57	1266	*T*(s) 61		1284
1241	*T*(m) 57	1244	*T*(m) 57		
772	*P*(s) 52	774	*P*(s) 52		787
B_1 *modes*					
1329	*W*(s) 54	1335	*W*(s) 56		1335
1264	*T*(s) 56	1271	*T*(s) 51	1265	
1235	*W*(m) 42	1240	*W*(m) 33		
1209	*T*(m) 27	1204	*T*(m) 35	1209	1203
864	*P*(m) 33	861	*P*(m) 37	864	846
794	*P*(s) 36	795	*P*(s) 36		788
B_2 *modes*					
1319	*W*(s) 40	1316	*W*(s) 34		1319
1282	*W*(m) 42	1290	*W*(m) 39		1286
1263	*T*(s) 62	1265	*T*(s) 68		
1143	*T*(m) 30	1164	*T*(m) 33	1149	1153
820	*P*(m) 20	821	*P*(m) 24		
765	*P*(s) 50	766	*P*(s) 50	775	788
B_3 *modes*					
1329	*W*(s) 53	1332	*W*(s) 53	1331	1334
1292	*W*(m) 57	1289	*W*(m) 60	1290	1314
1261	*T*(s) 64	1264	*T*(s) 67	1267	
1220	*W*(m) 34	1230	*W*(m) 32	1242	
864	*P*(m) 52	854	*P*(m) 44	864	
782	*P*(s) 47	782	*P*(s) 45	775	793

[a] Only the highest value is shown

for *T*(m) in s-PB were observed at 1203 cm^{-1} (B_1) and 1153 cm^{-1} (B_2). The 1203 cm^{-1} band is weak and obscure at room temperature. The 1153 cm^{-1} band maintains its intensity in the melt.

It is well known that a melted polyethylene specimen shows broad Raman spectral bands characteristic for conformational disorder and that the sharp zone-centre modes lose their intensities[12]. On the other hand, in the temperature dependence of Raman spectrum of s-PB, the strong bands maintained their frequencies in the melt as shown in *Figure 4b*, and satellite bands at 830, 860 and 1284 cm^{-1} became broad. Hence, the bands characteristic of the conformational disorder were not clearly found. However, the 830 and 860 cm^{-1} bands shifted to 817 and 865 cm^{-1}, respectively, and became very sharp at 77 K as shown in *Figure 5b* (bands marked with asterisks). These bands are assigned to *P*(m) at 820 cm^{-1} in the B_2 species and *P*(m) at 864 cm^{-1} in the B_1 and B_3 species of the calculated modes. On lowering the temperature, the observed frequencies approach the calculated ones and the line widths become sharp. Cornell and Koenig reported that the CCH bendings of the CH_2 group at 774, 824 and 875 cm^{-1} in isotactic poly(1-butene) of form I are sensitive to the helical angle of the main chain and to the conformation[6]. They calculated the frequencies of these modes for 3_1 of $(TG)_3$ and 10_3, 7_2, 11_3 and 4_1 of $(T_2G_2)_2$ helical conformations, and found that the calculated frequencies linearly depend on the helix angle and are related to the dispersion curve of the helix. In the present case of s-PB of form I, if the conformation deviates from $(T_2G_2)_2$ because of conformational disorder, the frequencies of the CCH modes may deviate from the calculated ones and become broad from analogy with isotactic poly(1-butene). So, the observed 830 and 860 cm^{-1} bands reflect the conformational orderliness.

In *Figure 6* the temperature dependence of infrared spectrum of s-PB, obtained a few days after casting, is

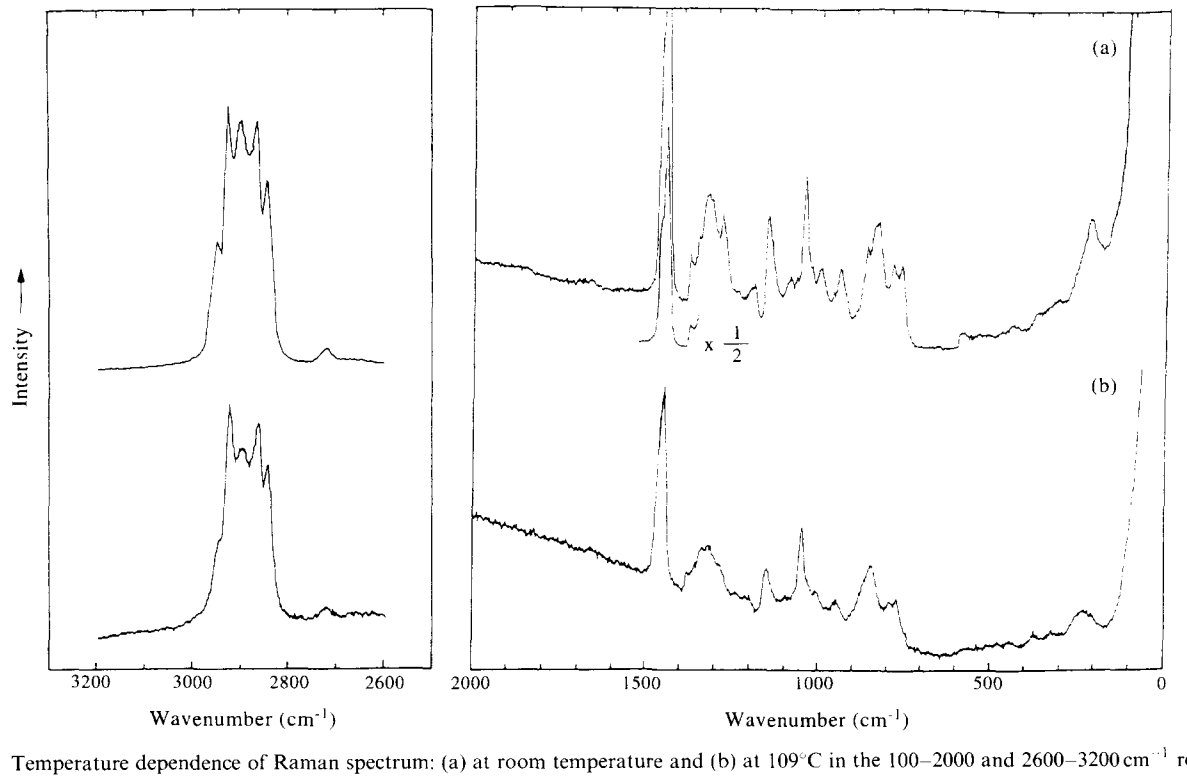

Figure 4 Temperature dependence of Raman spectrum: (a) at room temperature and (b) at 109°C in the 100–2000 and 2600–3200 cm^{-1} regions

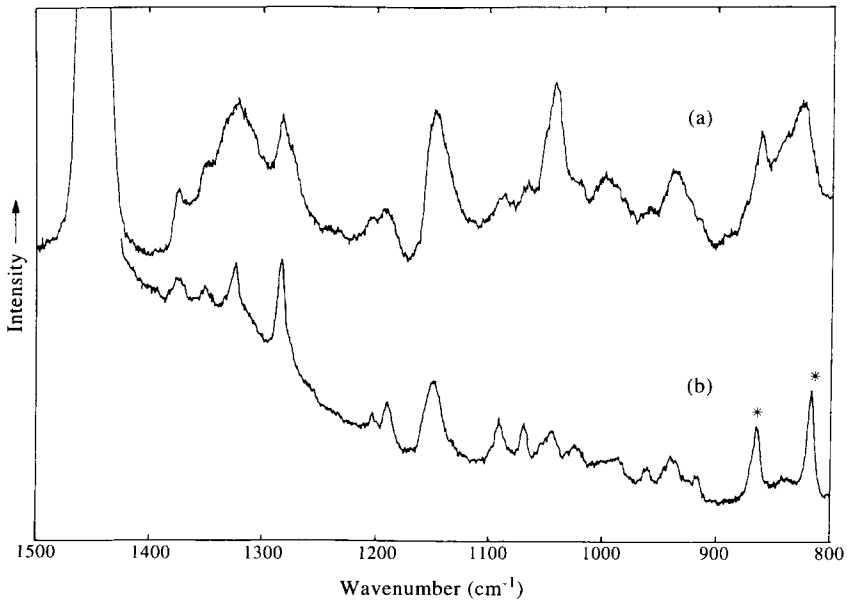

Figure 5 Temperature dependence of Raman spectrum: (a) at room temperature and (b) at 77 K in the 800–1500 cm^{-1} region. For an explanation of the bands marked with asterisks, see the text

shown. There is no prominent spectral change on going from 22 to 109°C (m.p. = 45°C). *Figure 7a* is the infrared spectrum at room temperature of a specimen 3 days after casting, *Figure 7b* is the spectrum at room temperature 11 days after casting, and *Figure 7c* is the spectrum at 75 K 55 days after casting. In contrast to the high-temperature spectra, sharp bands appear at (I) 863, 1209, 1241 and 1329 cm^{-1}, and at (II) 533, 931 and 997 cm^{-1} as shown in *Figures 7b* and *7c* with asterisks. The bands (I) are assigned to the CCH bendings of P(m), T(m), W(m) and W(s), respectively. The bands (II) are the CCC bendings and CC stretchings of ω(s), $S(m)^+$ and $S(m)^-$, respectively. If the conformation deviates from $(T_2G_2)_2$, the frequencies of the bands (I) may become broadly spread and apparently disappear, as in the case of above Raman bands. Hence, the infrared bands (I) are also sensitive to the conformation. In addition, the 1209 cm^{-1} band (I) of T(m) is a crystallinity sensitive band in the case of isotactic poly(1-butene) of form I as described above. To determine whether the band intensity is related to the degree of crystallinity or not, further experiments are needed.

In conclusion, the valence force field derived by Holland-Moritz was successfully applied to the s-PB of form I, although isotactic poly(1-butene) of form I

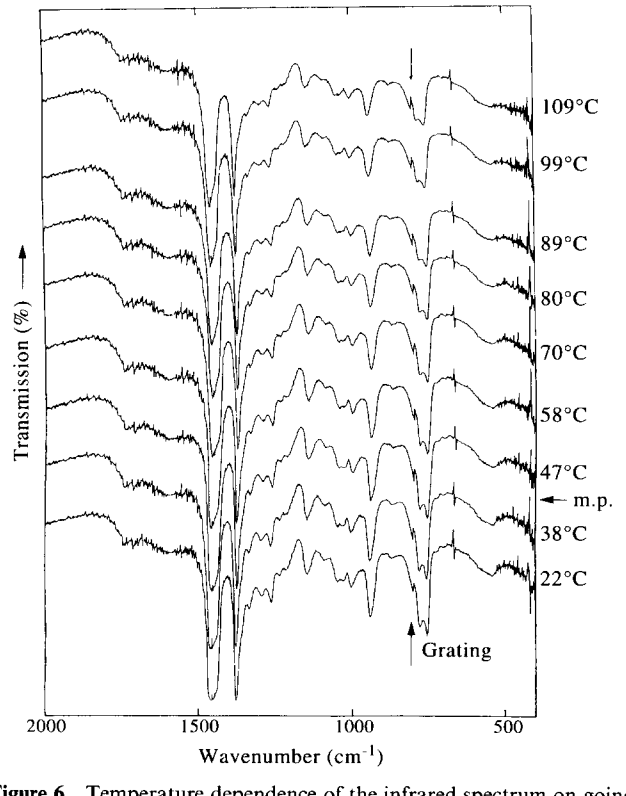

Figure 6 Temperature dependence of the infrared spectrum on going from 22 to 109°C in the 400–2000 cm^{-1} region

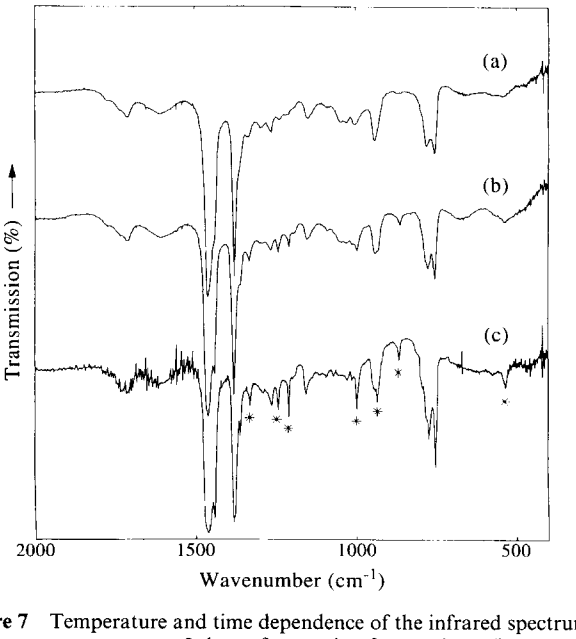

Figure 7 Temperature and time dependence of the infrared spectrum: (a) at room temperature 3 days after casting from xylene, (b) at room temperature 11 days after casting and (c) at 75 K 55 days after casting in the 400–2000 cm^{-1} region. For an explanation of the bands marked with asterisks, see the text

and s-PB of form I have different tacticity and conformations. The infrared and Raman spectra did not change in the melt but the CCH bendings of the spectra at low temperature were sensitive to the conformation. Generally, the vibrational bands of polymers are sensitive to the structure in the high-temperature region. In the present case of s-PB of form I, in contrast, the bands are found to be sensitive to the conformation at low temperature.

REFERENCES.

1. Ishioka, T., Murotani, S., Kanesaka, I. and Hayashi, S., *J. Chem. Phys.* 1995, **103**, 1999.
2. Chatani, Y., Maruyama, H., Noguchi, K., Asanuma, T. and Shiomura, T., *J. Polym. Sci., Polym. Lett. Ed.* 1990, **28**, 393.
3. Chatani, Y., Maruyama, H., Asanuma, T. and Shiomura, T., *J. Polym. Sci., Polym. Phys. Ed.* 1991, **29**, 1649.
4. Rosa, C. D., Venditto, V., Guerra, G., Pirozzi, B. and Corradini, P., *Macromolecules* 1991, **24**, 5654.
5. Holland-Moritz, K. and Sausen, E., *J. Polym. Sci., Polym. Phys. Ed.* 1979, **17**, 1.
6. 'Cornell, S. W. and Koenig, J. L., *J. Polym. Sci. A-2* 1969, **7**, 1965.
7. Ukita, M., *Bull. Chem. Soc. Jpn.* 1966, **39**, 742.
8. Abenoza, M. and Armengaud, A., *Polymer* 1987, **22**, 1341.
9. Luongo, J. P. and Salovey, R., *J. Polym. Sci. A-2* 1966, **4**, 997.
10. Schachtschneider, J. H. and Snyder, R. G., *Spectrochim. Acta* 1963, **19**, 117.
11. Schachtschneider, J. H. and Snyder, R. G., *Spectrochim. Acta* 1965, **21**, 1527.
12. Strobl, G. R. and Hagedorn, W., *J. Polym. Sci., Polym. Phys. Ed.* 1978, **116**, 181.